Received: 3 November 2021 | Accepted: 7 March 2022 | Published online: 14 April 2022

DOI: 10.1002/jeq2.20344

Journal of Environmental Quality

TECHNICAL REPORT

Surface Water Quality

Saturated buffer design flow and performance in Illinois

Janith Chandrasoma[1] | **Reid Christianson**[1] | **Richard Andrew Cooke**[2] | **Paul C. Davidson**[2] | **DoKyoung Lee**[1] | **Laura Christianson**[1]

[1]Dep. of Crop Sciences, Univ. of Illinois, Urbana-Champaign, IL 61801, USA

[2]Dep. of Agricultural and Biological Engineering, Univ. of Illinois, Urbana-Champaign, IL 61801, USA

Correspondence
Laura Christianson, Dep. of Crop Sciences, Univ. of Illinois, Urbana-Champaign, IL 61801, USA.
Email: lechris@illinois.edu

Assigned to Associate Editor Tyler Groh.

Funding information
Illinois Nutrient Research and Education Council, Grant/Award Number: Proj. No. 2017-4-360498-168

Abstract

There are few peer-reviewed studies documenting saturated buffer annual nitrate (NO_3) removal or that have assessed the federal practice standard design criteria. Drainage flow, NO_3, and dissolved reactive phosphorus (DRP) were monitored at three saturated buffers in Illinois, USA, for a combined 10 site-years. Nitrate loss reduction averaged 48 ± 19% with removals of 3.5–25.2 kg NO_3–N ha^{-1} annually. Median DRP concentrations at all sampling locations were at the analytical detection limit of 0.01 mg L^{-1}. The current design paradigm (i.e., USDA practice standard) prescribes there should be no flow bypassing the saturated buffer at flow rates that are ≤5% of the peak drainage system flow rate. The drainage coefficient–based and Manning's equation-based peak flow estimates were higher and lower, respectively, than the observed annual peaks in all years. This illustrated inherent uncertainty introduced early in the design process, which can be further compounded by dynamic in-buffer hydrology. The percentage of the observed peak flow rate at which bypass initiated ranged across an order of magnitude between sites (4.4–8.1% of peak flow rate at one site and 42–49% of peak at another) despite the buffers providing relatively similar NO_3 removal. Bypass at one site (SB2) was related to the concept of "antecedent buffer capacity filled," which was defined as the 5-d average water depth in the middle control structure chamber expressed as a relative percentage of the bypass stop log height. This design flow analysis serves as a call to further evaluate predictive relationships and design models for edge-of-field practices.

1 | INTRODUCTION

Saturated buffers (also called "saturated riparian buffers") are an edge-of-field mitigation technique for nitrate (NO_3) treatment in subsurface agricultural drainage. In this practice, a control structure is used to re-route drainage water laterally underground within the noncropped riparian buffer zone. A perforated distribution tile connected to the control structure allows the water to become hydrologically reconnected to the groundwater, where it can more slowly join the stream as base flow rather than via the tile drain outlet (Jaynes & Isenhart, 2014). Denitrification is thought to be the dominant process of NO_3 removal, and saturated buffers have been shown not to be large sources of nitrous oxide compared with cropped land (Davis et al., 2019; Groh et al., 2019). Considering the newness of this practice and the annual time-step required to develop NO_3 removal performance estimates, there are few peer-reviewed studies documenting saturated buffer annual NO_3 removal effectiveness. Indeed, a recent meta-analysis on nutrient mitigation measures for agricultural drainage could

Abbreviations: DRP, dissolved reactive phosphorus; SB, saturated buffer.

not perform statistical analyses on saturated buffers due to a lack of saturated buffer performance data (Carstensen et al., 2020).

Jaynes and Isenhart (2019a) provided the most comprehensive saturated buffer assessment to date with monitoring of six saturated buffers in Iowa, USA (17 full plus 2 partial site-years). Annual NO_3 loss assessed at the edge of the field ranged from 7 to 92% in individual years and averaged 44 ± 26% (median, 35%) across all site years. Their work was foundational for the inclusion of this practice as a recommended practice in the Iowa Nutrient Reduction Strategy in 2016 with a 50% annual NO_3 loss reduction (Iowa Department of Agriculture and Land Stewardship, Iowa Department of Natural Resources, and Iowa State University College of Agriculture and Life Sciences, 2017). Jacquemin et al. (2020) recently reported that a 500-m long saturated buffer in Ohio, USA, treated 25% of the annual drainage flow from a 55-ha field and generally reduced NO_3 concentrations in the monitoring well network to the analytical detection limit; however, no annual load reduction was calculated. Earlier proof-of-concept assessments of this technology reported NO_3 loss reduction of 23 ± 28% across 23 site-years, although a variety of sites (e.g., a variety of soil types, topographies, and vegetation) were intentionally assessed in that early study and some were found to be non-ideal (e.g., included coarse soil layers or insufficient soil carbon) (Utt et al., 2015).

To prevent conservation drainage practices from significantly reducing in-field drainage capacity, a portion of annual flow bypasses the saturated buffer. Jaynes and Isenhart (2019a) showed the percentage of flow treated by the saturated buffer in a given site-year tended to be a driver of the practice's NO_3 removal effectiveness. For example, at their BC-1 site in 2016, 50% of the NO_3 load from the field was diverted into the buffer, and the ultimate NO_3 removal effectiveness at the edge of the field was 48% in that year. Put differently, 13 of 19 (full and partial) site-years were reported to have >90% of the NO_3 load diverted to the buffer be removed. The natural processing of NO_3 in the buffer soil does not appear to be limiting the overall NO_3 removal performance of this practice for the sites evaluated thus far.

McEachran et al. (2020) took this a step further by modeling the theoretically ideal widths of saturated buffers post hoc with empirical performance data from Iowa. All of their sites were found to have been installed wider than would be necessary to maximize NO_3 removal given that narrower buffers allow for more water to be treated (at a given difference in head gradient between the control structure and the stream). Additional recent work from Iowa reported that routing water through a bank face at a saturated buffer may not cause significantly increased bank instability as previously thought (Dickey et al., 2021). Maximizing the amount of drainage flow treated (and thus the NO_3 load received) by a buffer clearly matters for the performance of this practice, and, accordingly, new variations of saturated buffer technology are investigating how to facilitate treatment of more drainage water (e.g., use of a second perforated distribution lateral; Jaynes & Isenhart, 2019b).

Core Ideas

- Three saturated buffers in Illinois provided an ≈50% annual reduction in NO_3 load.
- Observed peak flow rates differed from estimation methods used for design purposes.
- Two sites had relatively similar nitrate removals but different bypass trends.
- "Antecedent buffer capacity filled" was the water depth in the middle chamber as a percent of stop log height.

The USDA Natural Resources Conservation Service (USDA-NRCS) Conservation Practice Standard for Saturated Buffers (CPS Code 604), which sets the design criteria for saturated buffers installed through federal conservation programs, established that the flow rate used to design a saturated buffer should be no less than 5% of the of the drainage system capacity or as much as practical based on the available length of the vegetated buffer (USDA-NRCS, 2020). Despite the importance of maximizing the amount of flow and NO_3 load received by the buffer, there has been no published assessment of these design flow rates compared with observed saturated buffer performance.

Saturated buffers are an accepted NO_3 loss reduction practice for tile-drained landscapes of Iowa, but other states and regions are similarly working to reduce NO_3 loss from tile-drained agriculture. The overarching objective of this work was to assess the effectiveness of saturated buffers outside of Iowa, where foundational work has been done. A second, more design-oriented objective was to perform a flow analysis in context of the design criteria established by the NRCS Conservation Practice Standard for Saturated Buffers.

2 | MATERIALS AND METHODS

2.1 | Site descriptions

Three saturated buffers in Illinois were evaluated for nutrient loss reduction for a total of 10 site-years (Table 1; Supplemental Figures S1–S3). The first two sites (SB1 and SB2) were located on private farms and were established in existing Conservation Reserve Program grass buffers. The third site (SB3) was located near the University of Illinoi on a long-existing forested buffer. All saturated buffers received

TABLE 1 Site and design characteristics of three saturated buffers (SB1, SB2, and SB3) in Illinois

Characteristic	SB1	SB2	SB3
Year established as a buffer	1997	2000	2005 (estimated)
Year established as a saturated buffer	2016	2013	2018
Drained crop area, ha	9.9	6.9	11.9
Diameter of main pipe, cm	15.2	12.7	15.2
Buffer width, m	30	32	45 - 85
Buffer soil type	Radford silt loam	Radford silt loam, Sawmill silty clay loam	Elburn silt loam, Sawmill silty clay loam
Buffer vegetation	cool-season smooth bromegrass (*Bromus inermis* Leyss.)	cool-season smooth bromegrass	cool-season smooth bromegrass; perennial shrubs and trees
Length of lateral tiles, m	80 and 210 (two distribution lines)	396	300
Monitoring wells	9 (3 transects of 3)	9 (3 transects of 3)	none
30-yr average rainfall (1981–2010), mm	967	1,035	1,009

subsurface drainage water from fields that were under a corn (*Zea mays* L.) and soybean [*Glycine max* (L.) Merr.] rotation. Predominant soils at all three (Table 1) had restrictive layers at >2 m depth (USDA-NRCS, 2022).

The first site (SB1) received subsurface drainage from 9.9 ha into two distribution pipes extending from opposite sides of the control structure (80 and 210 m). The site had been a buffer since 1997 and was converted into a saturated buffer in 2016. The second site (SB2) was 1 of 15 original saturated buffer sites studied across the U.S. Midwest in 2013–2015 by Utt et al. (2015). It received subsurface drainage from 6.9 ha into a 396-m distribution tile. The site had been a buffer since 2000 and was converted into a saturated buffer in 2013. This site previously treated 91 and 13% of the flow from the field in 2014 and 2015, respectively, resulting in 83 and 4% annual NO_3 loss reductions in those years (Utt et al., 2015).

The third site (SB3) was constructed when a new 11.9-ha subsurface drainage system was installed for research on University of Illinois property in 2018. However, the buffer itself was not located on university property, and it was not possible to install monitoring wells despite efforts to work with the private landowner. Additionally, iterative management of the in-field drainage research at the site resulted in setting the saturated buffer stop logs relatively low to minimize the possibility of interference with the in-field research. Despite the lack of monitoring wells and non-ideal stop log settings, this site was included to provide a realistic low-end bound for this flow analysis. The buffer was assumed to be most similar to the 21-m wide BC1 from Jaynes and Isenhart (2019a) given SB3 was a mature treed buffer of at least 45 m. Given the lack of monitoring wells, NO_3 concentration reductions across the buffer for each sample event were assumed to be similar to that previously reported site (mean, 97% NO_3 removal for diverted NO_3 load, $n = 7$ site-years; Jaynes and Isenhart [2019a]).

Rainfall was measured at SB1 and SB2 using an on-site weather station equipped with a tipping bucket rain gauge (HOBO RX3000 station with S-RGA-M002 gauge, Onset Computer Corporation). Rainfall at SB3 was measured through a combination of weather stations (WatchDog, 2900ET, Spectrum Technologies and HOBO, RX3000, Onset Computer Corporation) located within 3 km of the site. Missing rainfall data were filled in from the nearest location of the NOAA/NWS Cooperative Observer Network obtained through the Midwestern Regional Climate Center (NWS COOP, 2021).

2.2 | Flow monitoring

The three-chamber diversion control structures (Supplemental Figure S4) at all sites were equipped with two water level data loggers (HOBO, U20L-04, Onset Computer Corporation), which recorded water levels at 15-min intervals in the first and middle chambers. Data were corrected for barometric pressure and any predetermined sensor offsets, compiled into daily water levels, and used to calculate flow using an appropriate weir equation. A V-notch weir equation was used to calculate flow rates at SB1 and SB2, with a compound weir equation used when the water level was higher than the depth of the "V" (see Supplemental Material for equations; equations provided by the manufacturer, Agri Drain Corp.). At SB3, a rectangular weir was used with the corresponding weir equation (Supplemental Material). Manual water levels were recorded during each site visit to validate logged pressures and water depths.

Flow data post-processing included setting conditions to address flooded conditions and when water was draining from the saturated buffer into the control structure (i.e., reverse flow for the saturated buffer). In the first condition, when the water level recorded above the bypass stop logs (i.e., the second set of stop logs in the control structure) was higher than the inflow stop log setting (the first set of stop logs), the structure was considered flooded, and all flow was assumed to be zero. Days of flooding were more common at SB3 compared with SB1 and SB2, with 11, 4, and 2% of total days monitored experiencing flooded conditions, respectively (Supplemental Table S1).

In the second condition (reverse flow), if the calculated bypass flow rate was larger than the flow rate entering the structure from the cropped field (thus indicating water was being drained from the saturated buffer area), the flow rate routed to the buffer was set to zero. The justification was that the water and nutrient evaluation boundary was for the tile drained field, not any groundwater entering the buffer then draining to the control structure. Under those conditions, the bypass flow rate was set equal to the inflow rate from the cropped field. Days of reverse flow were 5% or less of the total monitoring period across the three sites (Supplemental Table S2).

To explore bypass flow trends more deeply, a 5-d average "antecedent buffer capacity filled" term was defined as the average water depth in the middle chamber of the control structure (the chamber that fed the buffer) over the 5 d preceding the bypass flow initiation event. Expressing mean water depth relative to the height of the second set of stop logs (i.e., bypass stop logs) yielded this "capacity filled" term, which was comparable across sites because it ranged from 0 to 100%. For example, a 5-d average capacity filled of 90% meant that the water level in the middle chamber averaged 90% of the stop log height over the 5 d prior to the bypass event and that the buffer would have been considered relatively wet prior to the event. An antecedent capacity of 100% filled would be equivalent to bypass flow occurring because the water depth would be the height of the stop logs (or greater). A 5-d window was used in the analysis, which was consistent with antecedent runoff conditions associated with the NRCS Runoff Curve Number method (Chow et al., 1988). The bypass stop logs were set to 36 and 44 cm at SB1 and SB2, respectively, for the duration of the monitoring period.

2.3 | Nutrient monitoring and load calculation

Saturated Buffer 1 and SB2, but not SB3, had monitoring well networks for assessing nutrient removal across the buffer width (Supplemental Figures S1–S3). The well network at SB1 was installed to consist of four transects each with four wells, but the transect furthest from the control structure (182 m from the structure) received hydrologic influence from a different subsurface drainage system. This was visually corroborated by the discovery of an unsuspected nearby tile outlet. Additionally, the wells closest to the stream in the remaining three transects at SB1 were consistently dry. Thus, the monitoring well network at SB1 was functionally three transects with three wells each, where the wells were 5 m upgradient of the distribution tile and 5 and 10 m down gradient of the tile. The monitoring well network at SB2 was installed with three transects with three wells each, but the set of wells closest to the stream was often dry (5, 11, and 17 m downgradient of the tile) (Table 1). The average depth of the monitoring wells from the soil surface to the well point was 1.7 and 1.9 m for SB1 and SB2, respectively. Wells were screened for the bottom 1.4 m, but it was possible that flow moved beneath the wells given the depth to the restricting layer was >2 m (USDA-NRCS, 2022).

Water samples at SB1 and SB2 were collected from the control structure, monitoring wells, and stream (upstream of the saturated buffer outlet) every 2–3 wk during flow periods. The monitoring wells were purged with a battery-powered submersible pump (WSP-12V-1 Cyclone, Waterra) and allowed to refill prior to sampling. Water samples were stored on ice for transport, filtered within 48 h with 0.45-µm filters, and kept frozen until analysis, which was within 1–8 mo. The water samples were analyzed for NO_3–N and dissolved reactive phosphorous (DRP) using analytical detection limits of 0.10 mg NO_3–N L^{-1} and 0.01 mg P L^{-1}, respectively (Methods 10-107-04-1-A and 10-115-01-1; QuikChem 8000, Lachat).

The average concentration from the set of wells closest to the stream that consistently provided samples was used as the saturated buffer outlet concentration for each sample event, following Jaynes and Isenhart (2019a). This was the set of wells 10 and 11 m downgradient of the distribution line at SB1 and SB2, respectively. The saturated buffer inlet concentration (in the control structure) and this outlet concentration were each multiplied by the incremental flow volume that had been diverted to the saturated buffer because the previous sample event to calculate incremental nitrogen (N) and phosphorus (P) loads routed into and out of the buffer. Jaynes and Isenhart (2019a) acknowledged "This is a rather crude estimate of mass removal…" with a handful of assumptions about uniform flow and loading across the buffer. Nevertheless, this was the most defensible way to cost-effectively monitor and develop NO_3 removal effectiveness values for saturated buffers.

The flow routed into the buffer was not directly measured; rather, this flow was estimated as the difference between the total flow coming from the cropped field and the flow bypassing to the stream, following Jaynes and Isenhart (2014). The nutrient loads that bypassed the buffer to the stream were

TABLE 2 Drainage and buffer water balance for 10 saturated buffer site-years (three sites) in Illinois

Site	Water year	Rainfall	Drainage	Rainfall as drainage	To buffer	Flow diverted into buffer
		mm	mm	%	mm	%
SB1	2019	1,039	145	14	32	22
	2020	656	216	33	163	76
	2021	740	110	15	58	53
SB2	2018[a]	422	79	19	63	80
	2019	1,050	210	20	86	41
	2020	881	319	36	189	59
	2021	805	129	16	81	63
SB3	2019	974	227	23	177	78
	2020	965	362	37	206	57
	2021	788	310	39	164	53

[a]Partial water year: 15 Mar. 2018–30 Sept. 2018 rather than 1 Oct. 2017–30 Sept. 2018.

calculated using nutrient concentrations sampled in the control structure and the incremental flow volumes that bypassed. Incremental loads for each sample event were summed to develop annual values.

The residuals of the nutrient concentrations at a given sampling location were non-normally distributed based on Shapiro–Wilk tests (Sigma Plot version 14.0, Systat Software, Inc.). Therefore, comparisons between locations were made using Kruskal–Wallis one-way ANOVA on ranks.

3 | RESULTS AND DISCUSSION

3.1 | Water quality improvement

The percentage of flow treated by the three saturated buffers across 10 site-years was a driver for these sites' ultimate annual NO_3 loss reduction percentages. For example, SB1 treated 22, 76, and 53% of the drainage water in 2019, 2020, and 2021, respectively (Table 2), and provided 19, 73, and 46% NO_3 loss reduction in 3 yr (Table 3). This was also illustrated through the relatively effective NO_3 reduction provided by the buffers, which removed more than half of the N that was routed into them; often more than 75% of the diverted NO_3 loss was removed (Table 3; note the assumptions made about SB3 where there were no monitoring wells). McEachran et al. (2020) numerically demonstrated the importance of the percentage of flow treated by showing that, when saturated buffer outlet nitrate concentrations approach zero (e.g., Figure 1a in SB1's monitoring wells), overall buffer nitrate removal effectiveness is a function of flow treated.

The mean ± SD NO_3 loss reduction across the 10 site-years was 48 ± 19% (median, 47%; means for SB1, SB2, and SB3 were 46, 40, and 60%, respectively) (Table 3). These NO_3 loss reductions ranged from 3.5 to 25.2 kg NO_3–N ha-yr^{-1} (34–300 kg yr^{-1} NO_3–N removed) (Table 3). Summing the total mass from the field from all 10 site-years (2,392 kg NO_3–N) and total mass removed by the saturated buffers (1,167 kg NO_3–N) resulted in a practice efficiency of 49% NO_3 load reduction. These efficiencies were very consistent with the practice efficiency value of 50% recommended for saturated buffers in the Iowa Nutrient Reduction Strategy (Iowa Department of Agriculture and Land Stewardship, Iowa Department of Natural Resources, & Iowa State University College of Agriculture and Life Sciences, 2017).

Comparing individual sites showed that SB1 tended to have lower subsurface drainage NO_3 concentrations compared with SB2 and SB3, with NO_3 concentrations in the control structure exceeding 20 mg NO_3–N L^{-1} five and four times at SB2 and SB3, respectively (Supplemental Figures S5b and S7b). Correspondingly, the highest annual NO_3 losses (>27 kg NO_3–N ha^{-1}) and loads (>330 kg NO_3–N) from the field occurred at SB2 in 2020 and at SB3 in all years (Table 3).

There were also differences between years, with the 2019 water year being the wettest (i.e., highest precipitation) at all sites (Table 2). Post-processing flow data in this year required excluding a number of events due to flooding and reverse flow (Supplemental Tables S1 and S2). Although this approach introduces some uncertainty, it is a realistic and inherent limitation of monitoring edge-of-field practices that are necessarily placed in low areas near streams or ditches. Regardless, 2019 was the only year where less than 50% of the flow from the field was diverted into SB1 and SB2 (Table 2; Supplemental Figures S5a and S6a). On-site flooding would have affected in-buffer hydrology where saturated buffer soils and a reduced hydraulic gradient due to the stream being high might have limited the buffer's ability to receive drainage from the field. The flow trends in 2019 were in contrast with those in 2020, where more than 160 mm of drainage was diverted into both buffers (Table 2; Supplemental Figures S5a and S6a).

TABLE 3 Nitrogen loss and removal metrics for 10 saturated buffer site-years (three sites) in Illinois

Site	Water year	Annual flow-weighted NO_3–N concentration	NO_3 loss from the field	NO_3 loss diverted into the buffer	NO_3 loss diverted into the buffer	NO_3 loss removed by the buffer	NO_3 load removed by the buffer	Diverted NO_3 loss removed by the buffer	NO_3 loss from the field removed	Site NO_3 loss removed (mean ± SD)
		mg L^{-1}	kg ha^{-1}		%	kg ha^{-1}	kg	%		
SB1	2019	13.0	18.0	3.8	21	3.5	34	91	19	
	2020	5.8	11.3	8.5	75	8.3	82	97	73	
	2021	11.7	14.9	8.2	55	6.9	68	84	46	46 ± 27
SB2	2018[a]	17.7	13.9	11.1	80	8.6	59	77	61	
	2019	12.4	26.0	11.5	44	7.3	50	63	28	
	2020	16.0	49.7	29.7	60	17.0	117	57	34	
	2021	19.7	26.8	17.5	65	9.5	66	54	36	40 ± 15
SB3	2019	15.4	32.6	26.0	80	25.2	300	97[b]	77	
	2020	10.0	36.2	20.1	56	19.5	232	97[b]	54	
	2021	9.3	27.8	13.8	49	13.3	159	97[b]	48	60 ± 16

[a]Partial water year: 15 Mar. 2018–30 Sept. 2018.

[b]Assumed from Jaynes and Isenhart (2019a) BC-1 site, used to calculate NO_3 loss removed in the buffer.

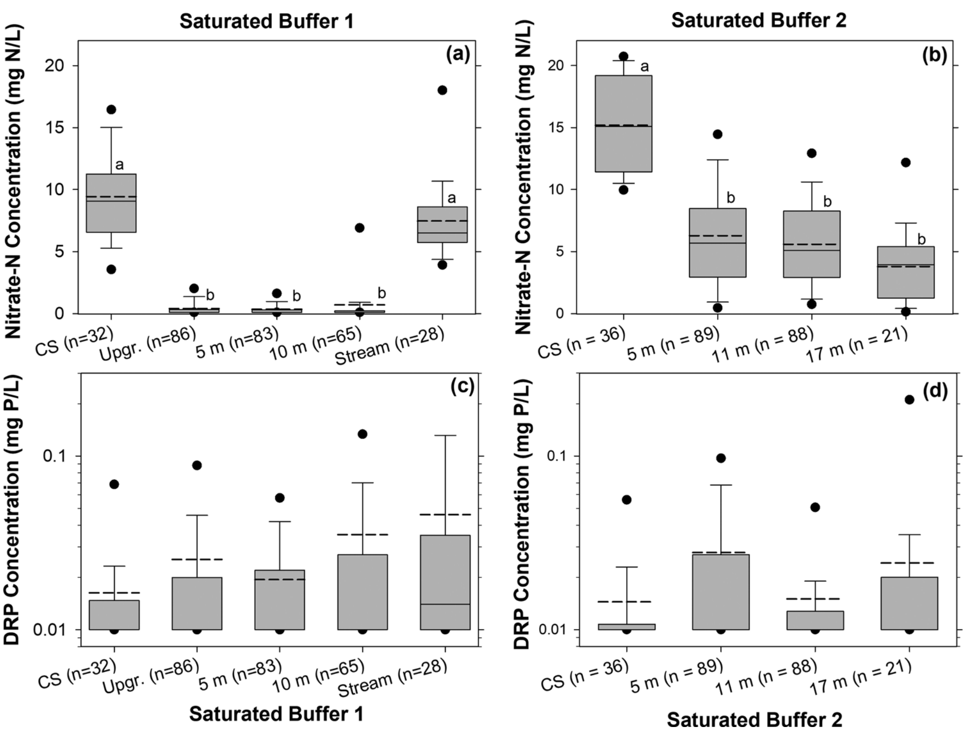

FIGURE 1 Range of (a, b) NO_3–N concentrations and (c, d) dissolved reactive P (DRP) concentrations in the control structure (CS) and monitoring wells at specified distances downgradient from the distribution lateral at (a, c) SB1 and (b, d) SB2. “n” is the number of discrete grab samples per location over the multi-year monitoring period. It was also possible to collect samples in the stream (“Stream”) and upgradient of the distribution tile (“Upgr.”) at SB1. Boxes, stems, and dots represent the 25th and 75th, 10th and 90th, and 5th and 95th percentiles, respectively; the solid and dashed lines are the median and mean, respectively. Boxes with the same letter within a given panel are not statistically significantly different (α = .05)

There was relatively less rainfall in the latter year, with relatively more measured drainage (>30% of precipitation) and more successfully diverted flow into the buffer (Table 2).

Control structure and well samples were analyzed for DRP in addition to NO_3, but the twice-monthly sampling events introduced an unacceptable level of uncertainty in estimating annual P loss trends (e.g., greater than ±25% uncertainty) (Williams et al., 2015). It was also unclear if the well samples were providing an accurate representation of DRP concentrations in the water being transmitted through the buffer rather than a representation of DRP dissolving into solution due to the soil (and associated soil test P) immediately around the well or soil particles that had fallen inside the wells. Nevertheless, the median DRP concentrations across the monitoring period for samples collected in the control structure and wells at three distances from the distribution tile at SB1 were all 0.01 mg DRP L^{-1} (the analytical detection limit; Kruskal–Wallis ANOVA: $p = .242$) (Figure 1c). The same DRP median values of 0.01 mg P L^{-1} were observed at SB2 monitoring locations (Figure 1d). Dissolved P concentration reductions were reported for a saturated buffer in Ohio, but the concentrations in the control structure averaged 0.08 mg DRP L^{-1} (Jacquemin et al., 2020), which was higher than either site with monitoring wells here (mean ± SD of 0.02 ± 0.02 [n = 32] and 0.01 ± 0.01 mg DRP L^{-1} [n = 36] for SB1 and SB2 control structures, respectively). Bryant et al. (2019) recommended this be an area for future research for saturated buffer implementation in the Chesapeake Bay watershed, and although some additional insight is provided here in that no change in DRP concentrations across the saturated buffers was observed, there are still many unknowns.

Differences in NO_3 concentrations between the control structure and monitoring well network at both sites were significant (Kruskal–Wallis ANOVA: $p < .001$ for both sites) (Figure 1a,b). For example, median NO_3 concentrations over the entire monitoring period at SB2 decreased from 15.1 mg NO_3–N L^{-1} in the control structure to 5.68, 5.09, and 3.94 mg NO_3–N L^{-1} for the wells at increasing distance from the distribution lateral (Figure 1b). However, the concentrations at the three distances from the lateral tile were not statistically significantly different, which indicated that NO_3 removal benefits happen early along the buffer gradient, as has been observed previously (e.g., Jaynes & Isenhart, 2014, 2019a).

3.2 | Design and bypass flow analysis

Jaynes and Isenhart (2019a) reported that annual mass NO_3 removal by saturated buffers in Iowa was most strongly correlated with the product of drainage area and distribution pipe length. Although SB1 and SB2 related well to this previously reported relationship, two of the SB3 site-years trended higher (Figure 2). Saturated Buffer 3 was a unique three-way combination of (a) the largest drainage area of the three sites (11.9 ha), (b) some of the highest NO_3–N concentrations and consistently high loading (Supplemental Figure S7; Table 3), and (c) the most mature and widest buffer. A 97% NO_3–N removal for water diverted into SB3 was assumed because it was not possible to install monitoring wells. However, even assuming a lower removal would have still resulted in two of the three SB3 points being notably high in Figure 2 (e.g., assuming 60% removal still yielded >140 kg NO_3–N yr^{-1} removed for two site-years). Nevertheless, these new data support the previous finding by Jaynes and Isenhart (2019a): "This intuitive finding suggests that to remove the most NO_3, the drainage area going to the tile outlet and the SRB length [length of distribution pipe] should be maximized."

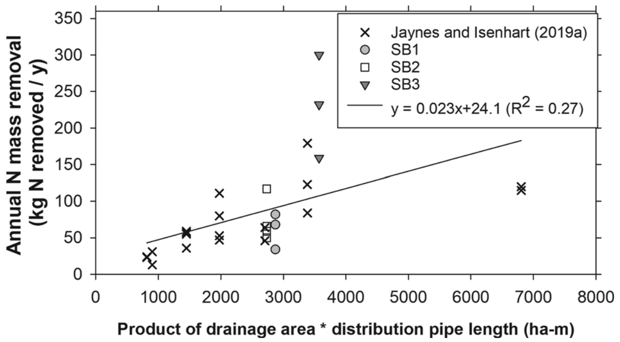

FIGURE 2 Predictive relationship between saturated buffer (SB) drainage area, distribution pipe length, and annual mass N removal from Jaynes and Isenhart (2019a) updated with 10 site-years from three Illinois saturated buffers (SB1, SB2, SB3)

The NRCS Conservation Practice Standard for Saturated Buffers states: "Minimum saturated buffer design flow is 5 percent of drainage system capacity or as much as practical based on the available length of the vegetated buffer" (USDA-NRCS, 2020). This means a saturated buffer should treat 100% of the flow from the field (i.e., no bypass flow should be occurring) when the drainage system is operating at a flow rate that is ≤5% of the estimated peak. Peak drainage system flow rates are commonly estimated for design purposes using the drainage coefficient method (estimated drainage area × the design drainage coefficient) or Manning's equation assuming full pipe flow. Observed peak drainage system flow rates across the 10 site-years were all lower than the typical drainage coefficient for these fields (Drablos & Moe, 1984) and higher than the Manning's equation-estimated peak (Table 4; assuming 0.1% grade for all sites). These data illustrate the challenge of accurately and reliably estimating an appropriate peak flow rate for use in the design of edge-of-field drainage water quality improvement practices.

One way to maximize annual NO_3 removal at a saturated buffer is to maximize the amount of flow treated, meaning a design aim could be to minimize bypass flow. This could be done by maximizing the flow rate at which bypass

TABLE 4 Drainage system flow rates when saturated buffer bypass flow initiated in context of the peak drainage system flow rates (observed, drainage coefficient, and Manning's equation-based methods) for 10 site-years (three sites) in Illinois

Site	Water year	Bypass events (n)	Drainage system flow rate at bypass initiation: Mean ± SD	Drainage system flow rate at bypass initiation: Median	Drainage system peak flow rate: Observed	Drainage system peak flow rate: Drainage coefficient	Drainage system peak flow rate: Manning's	Peak flow rate at which bypass flow initiated: Observed	Peak flow rate at which bypass flow initiated: Drainage coefficient	Peak flow rate at which bypass flow initiated: Manning's
			mm d^{-1}					%		
SB1	2019	16	0.31 ± 0.20	0.28	7.1	9.5	3.8	4.4	3.3	8.3
	2020	18	0.57 ± 0.75	0.33	7.1	9.5	3.8	8.1	6.0	15
	2021	22	0.47 ± 0.40	0.50	7.1	9.5	3.8	6.6	4.9	12
SB2	2018[a]	3	1.5 ± 0.48	1.4	3.5	9.5	3.3	42	15	44
	2019	9	2.5 ± 1.1	2.3	5.7	9.5	3.3	43	26	74
	2020	10	2.6 ± 0.49	2.6	6.0	9.5	3.3	43	27	77
	2021	4	3.4 ± 0.29	3.5	7.0	9.5	3.3	49	36	102
SB3	2019	15	1.3 ± 0.43	1.3	4.5	9.5	3.2	29	14	41
	2020	10	0.77 ± 0.19	0.80	5.5	9.5	3.2	14	8.1	24
	2021	5	1.0 ± 0.40	1.1	5.3	9.5	3.2	19	11	31

[a]Partial water year: 15 Mar. 2018–30 Sept. 2018.

initiates. Conceptually, if bypass initiates later during a given flow event (i.e., at a higher flow rate from the field), relatively more water will be routed into the buffer for that event. This amount of water treated during a given event is affected not just by set parameters of the distribution tile length and the soil physical characteristics; it also could be limited by dynamic factors, including antecedent moisture conditions of the buffer soil, flashiness of drainage flow from the field, and the hydraulic gradient across the buffer (e.g., how boards are set and stream depth) (McEachran et al., 2020). In other words, there are dynamic physical boundaries regarding the ability of the buffer to receive water from the lateral distribution pipe when the soil is saturated vs. dry, or the stop logs or receiving stream are high or low. These relationships are not yet well understood in saturated buffers.

For each drainage hydrograph where bypass flow initiated at these three saturated buffers, the flow rate from the field at the time bypass initiated was interpolated from the 15-min pressure transducer data. In other words, the flow rate over the first set of stop logs was determined for every time flow over the second set of stop logs started for a given bypass event. There were between 3 and 22 bypass flow events per year across the three sites, and differences between sites were more notable than differences between years (Table 4). For example, bypass flow events initiated at lower flow rates from the field and were more numerous at SB1 compared with the other two sites. This bypass flow analysis was limited at SB3 due to the low stop log settings; this control structure was adjusted once (related to the ongoing in-field research; see Materials and Methods), and differences in bypass initiation flow rates due to the stop log management were observed, as would be expected.

Only one site-year had mean bypass flow initiate at a flow rate from the field that was <5% of the peak drainage system capacity (SB1 in 2019 for both observed and drainage coefficient peak estimation methods) (Table 4). This bypass flow analysis highlighted that the percentage of the observed peak flow rate that was entirely routed into SB1 was much lower than at SB2 at 4.4–8.1 vs. 42–49%, respectively. This notable difference may have been related to the timing of their installations (Table 1) because SB2 was designed and installed in 2013 prior to the release of the interim Conservation Practice Standard in 2016 that provided design flow guidance. Nevertheless, SB1 and SB2 provided relatively similar ranges of annual NO_3 loss reduction effectiveness (19–73 and 28–61%, respectively) (Table 3) and overall mass of NO_3 removed (34–82 and 50–117 kg NO_3–N) (Table 3; Figure 2).

These data illustrated that bypass flow does not initiate at a consistent flow rate from the field for every event, even though the control structure stop log settings were not modified over the monitoring period at SB1 or SB2 (Table 4; Figure 3). The flow rate from the field at which bypass flow initiated at SB2 was related to the antecedent moisture in the buffer, as assessed by a 5-d average "antecedent buffer capacity filled" term (Figure 3). When SB2 was wetter (i.e., had more of the buffer capacity filled over the preceding 5 d), bypass flow initiated at lower flow rates from the field drainage system (Figure 3). Conceptually, when that buffer was wet, it could not receive as much incoming water from the field, and that water would be forced to bypass. The same trend with antecedent buffer capacity filled was not observed at SB1 (Figure 3). Although there was variability in bypass initiation flow rates at SB1, these events were not related to the capacity filled.

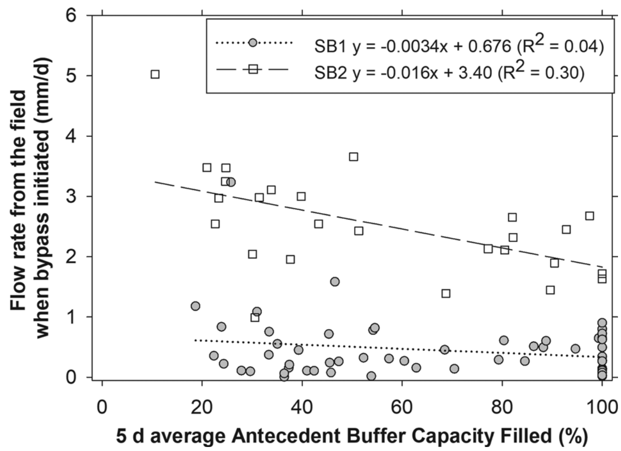

FIGURE 3 Drainage system flow rate from the cropped field at which bypass flow events initiated vs. the "antecedent buffer capacity filled" concept. This was defined as the 5-d average water depth in the middle control structure chamber expressed as a relative percentage of the stop log height. An antecedent buffer capacity filled of 100% is equivalent to bypass flow occurring. SB, saturated buffer

Nearly all bypass flow events had at least 20% of the antecedent buffer capacity filled prior to the event (Figure 3). If this had been 0%, the water table would have been below the distribution line, but that was never observed here on average over 5-d prior to a bypass event. One important nuance with this capacity concept is that conditions may exist such that a buffer is relatively dry (i.e., low antecedent capacity filled), but, after a large rainfall event that initiates significant drainage, the buffer's ability to infiltrate flow from the distribution line could be limited by the soil's hydraulic conductivity even though the buffer had available capacity. This nuance may explain the variation in the bypass initiation flow rates observed here (Table 4). This observed variability in bypass trends highlighted a knowledge gap involving drivers of internal buffer hydrology, which could affect saturated buffer design and should be further explored at additional sites.

4 | CONCLUSIONS

Although saturated riparian buffers are still considered a relatively new practice and there are few published annual performance estimates, the observed ∼50% NO_3 loss reduction from 10 saturated buffer site-years in Illinois was consistent with values from Iowa. The relatively infrequent sampling did not support defensible estimates of annual P loss reduction at these saturated buffers, and thus, based on these data, this practice cannot be recommended for this P loss purpose. Dissolved P concentrations in the control structures and monitoring wells tended to be the lower detection limit (i.e., median values were most often 0.01 mg DRP L^{-1}) with no trend across the buffer.

This analysis generally validated that saturated buffers in Illinois were operating consistently with the USDA-NRCS Conservation Practice Standard design criteria (i.e., 5% of peak) and provided good performance (e.g., ∼50% NO_3 removal). However, bypass events at SB2 were driven, in part, by the antecedent buffer capacity filled, which was defined as the 5-d average water depth in the middle control structure chamber expressed as a relative percentage of the bypass stop log height. This trend of bypass occurring at lower flow rates from the field when the buffer capacity was relatively more "filled" was not observed at SB1.

The marked differences in bypass events and initiation flow rates between sites and the relative lack of consistency in these bypass initiation flow rates between years raised the question of whether there may be a simpler saturated buffer design method. For example, constructed wetlands for treatment of subsurface drainage are often designed based on a percentage of the drainage area (e.g., wetland pool 0.5–2% of watershed area; Iovanna et al., 2008). Figure 2 contains a similar, relatively simple, area-based concept that could be useful if further validated with additional site-years of saturated buffer performance. In the current method, there are inherent limitations of estimating a drainage system peak flow rate (e.g., observed peak vs. drainage coefficient method) that introduce uncertainty early in the design process. That uncertainty is compounded by dynamic in-buffer hydrology, which helps drive the ability of the buffer to receive flow vs. bypass the flow. Despite differences, these three saturated buffers in Illinois performed well and demonstrated this new conservation practice outside of Iowa. Given the immense water quality improvement goals in the heavily tile-drained upper Mississippi River Basin, this work is a call to further evaluate predictive performance relationships and design models for edge-of-field conservation drainage practices with the aim of streamlining design and implementation.

ACKNOWLEDGMENTS

The authors thank the two private landowner families and their farm managers, whose willingness for us to undertake this research essentially underpinned the success of this study. We also thank Dr. Greg McIsaac, Tim McMahon, and Steve John for the partnership at SB2. The authors acknowledge additional research staff who assisted in the field and laboratory: Jack Mrozek, Ronnie Chacon, Fernando Zucher, Jazmine Rodriguez, Jason Kandume, Daniel Hiatt, and Michael Wallace. Funding was provided by the Illinois Nutrient Research and Education Council (IL NREC) Proj. No. 2017-4-360498-168: Drainage water management and saturated buffers for achieving NLRS goals.

AUTHOR CONTRIBUTIONS

Janith Chandrasoma: Data curation; Investigation; Writing – original draft. Reid Christianson: Conceptualization; Data curation; Formal analysis; Methodology; Supervision; Writing – review & editing. Richard Andrew Cooke: Conceptualization; Funding acquisition; Resources; Writing – review & editing. Paul C. Davidson: Conceptualization; Funding acquisition; Supervision; Writing – review & editing. Dokyoung Lee: Data curation; Investigation; Methodology; Writing – review & editing. DoKyoung Lee: Data curation; Investigation; Methodology; Writing – review & editing. Laura Christianson: Conceptualization; Formal analysis; Funding acquisition; Methodology; Project administration; Supervision; Validation; Visualization; Writing – review & editing.

CONFLICT OF INTEREST

The authors declare no conflict of interest.

ORCID

Laura Christianson https://orcid.org/0000-0002-2583-6432

REFERENCES

Bryant, R., Baldwin, A., Cahall, B., Christianson, L., Jaynes, D., Penn, C., & Schwartz, S. (2019). *Best management practices for agricultural ditch management in the Phase 6 Chesapeake Bay watershed model*. Chesapeake Bay Program. https://www.chesapeakebay.net/channel_files/31811/ag_ditches_bmp_panel_report_draft_for_cbp_review_04sep2019.pdf

Carstensen, M. V., Hashemi, F., Hoffmann, C. C., Zak, D., Audet, J., & Kronvang, B. (2020). Efficiency of mitigation measures targeting nutrient losses from agricultural drainage systems: A review. *Ambio*, *49*, 1820–1837. https://doi.org/10.1007/s13280-020-01345-5

Chow, V. T., Maidment, D. R., & Mays, L. W. (1988). *Applied hydrology*. McGraw-Hill.

Davis, M. P., Groh, T. A., Jaynes, D. B., Parkin, T. B., & Isenhart, T. M. (2019). Nitrous oxide emissions from saturated riparian buffers: Are we trading a water quality problem for an air quality problem? *Journal of Environmental Quality*, *48*(2), 261–269. https://doi.org/10.2134/jeq2018.03.0127

Dickey, L. C., McEachran, A. R., Rutherford, C., Rehmann, C. R., Perez, M. A., Groh, T. A., & Isenhart, T. (2021). Slope stability of streambanks at saturated riparian buffer sites. *Journal of Environmental Quality*, *50*(6), 1430–1439. https://doi.org/10.1002/jeq2.20281

Drablos, C. J. W., & Moe, R. C. (1984). *Illinois drainage guide – Circular 1226*. University of Illinois at Urbana-Champaign.

Groh, T. A., Davis, M. P., Isenhart, T. M., Jaynes, D. B., & Parkin, T. B. (2019). In situ denitrification in saturated riparian buffers. *Journal of Environmental Quality*, *48*(2), 376–384. https://doi.org/10.2134/jeq2018.03.0125

IDALS, IDNR, and ISU College of Agriculture and Life Sciences. Iowa Department of Agriculture and Land Stewardship, Iowa Department of Natural Resources, & Iowa State University College of Agriculture and Life Sciences. (2017). *Iowa nutrient reduction strategy: A science and technology-based framework to assess and reduce nutrients to Iowa waters and the Gulf of Mexico*. http://www.nutrientstrategy.iastate.edu/sites/default/files/documents/2017%20INRS%20Complete_Revised%202017_12_11.pdf

Iovanna, R., Hyberg, S., & Crumpton, W. (2008). Treatment wetlands: Cost-effective practice for intercepting nitrate before it reaches and adversely impacts surface waters. *Journal of Soil and Water Conservation*, *63*, 14A–15A. https://doi.org/10.2489/jswc.63.1.14A

Jacquemin, S. J., McGlinch, G., Dirksen, T., & Clayton, A. (2020). On the potential for saturated buffers in northwest Ohio to remediate nutrients from agricultural runoff. *PeerJ*, *8*, e9007. https://doi.org/10.7717/peerj.9007

Jaynes, D. B., & Isenhart, T. M. (2014). Reconnecting tile drainage to riparian buffer hydrology for enhanced nitrate removal. *Journal of Environmental Quality*, *43*, 631–638. https://doi.org/10.2134/jeq2013.08.0331

Jaynes, D. B., & Isenhart, T. M. (2019a). Performance of saturated riparian buffers in Iowa, USA. *Journal of Environment Quality*, *48*(2), 289–296. https://doi.org/10.2134/jeq2018.03.0115

Jaynes, D. B., & Isenhart, T. M. (2019b). Increasing infiltration into saturated riparian buffers by adding additional distribution pipes. *Journal of Soil and Water Conservation*, *74*(6), 545–553. https://doi.org/10.2489/jswc.74.6.545

McEachran, A. R., Dickey, L. C., Rehmann, C. R., Groh, T. A., Isenhart, T. M., Perez, M. A., & Rutherford, C. J. (2020). Improving the effectiveness of saturated riparian buffers for removing nitrate from subsurface. *Journal of Environmental Quality*, *49*(6), 1624–1632. https://doi.org/10.1002/jeq2.20160

National Weather Service (NWS) Cooperative Observer Program (NWS COOP). (2021). Midwestern Regional Climate Center. https://mrcc.purdue.edu/

USDA Natural Resources Conservation Service (USDA-NRCS). (2020). *Conservation practice standard-saturated buffer: Code 604*. https://www.nrcs.usda.gov/wps/PA_NRCSConsumption/download?cid=nrcseprd1051806&ext=pdf

Soil Survey Staff. USDA Natural Resources Conservation Service (USDA-NRCS). (2022). *Web soil survey*. http://websoilsurvey.sc.egov.usda.gov/

Utt, N., Jaynes, D., & Albertsen, J. (2015). *Demonstrate and evaluate saturated buffers at field scale to reduce nitrates and phosphorus from subsurface field drainage systems*. https://www.fsa.usda.gov/Assets/USDA-FSA-Public/usdafiles/EPAS/natural-resouces-analysis/pdfs/admc_final_report.pdf

Williams, M. R., King, K. W., Macrae, M. L., Ford, W., Van Esbroeck, C., Brunke, R. I., English, M. C., & Schiff, S. L. (2015). Uncertainty in nutrient loads from tile-drained landscapes: Effect of sampling frequency, calculation algorithm, and compositing strategy. *Journal of Hydrology*, *530*, 306–316. https://doi.org/10.1016/j.jhydrol.2015.09.060

SUPPORTING INFORMATION

Additional supporting information may be found in the online version of the article at the publisher's website.

How to cite this article: Chandrasoma, J., Christianson, R., Cooke, R. A., Davidson, P. C., Lee, D., & Christianson, L. (2022). Saturated buffer design flow and performance in Illinois. *Journal of Environmental Quality*, *51*, 389–398. https://doi.org/10.1002/jeq2.20344